Amphiphilic Azobenzenesulfonic Acid Anionic Surfactant for Water-Soluble, Ordered, and Luminescent Polypyrrole Nanospheres

M. Jinish Antony and M. Jayakannan*

Polymer Research Group, Chemical Sciences and Technology Division, National Institute for Interdisciplinary Science and Technology (Formerly: Regional Research Laboratory), Thiruvananthapuram 695019, Kerala, India

Received: July 6, 2007; In Final Form: August 23, 2007

Self-organized micelles of new renewable resource amphiphilic azobenzenesulfonic acid anionic surfactant were utilized to prepare water-soluble, luminescent, and highly ordered polypyrrole nanomaterials. The micellar behavior of the reaction medium was precisely controlled by varying the composition of pyrrole/surfactant ratio from 3 to 100 (up to 100 times lower amount of surfactant with respect to pyrrole), and polypyrrole nanospheres of 150−800 nm were prepared. Dynamic light scattering (DLS) and viscosity techniques were employed as tools to trace the factors, which control the mechanism of polypyrrole nanomaterials formation. DLS studies confirmed that the surfactant exists as in the form of spherical micelles of 4.8 nm diameter in water. Specific viscosity measurement revealed that the pyrrole+surfactant complexes in water exist in the form of either aggregated or isolated micelles depending upon their composition in the feed. SEM and TEM analysis confirmed that the aggregated micellar templates produced coral-like morphology, whereas uniform polypyrrole nanospheres of 150−400 nm were obtained at low micellar concentration. The nanomaterials formation was unperturbed by the variation of the oxidation agents such as ammonium persulphate (APS) or ferric chloride ($FeCl_3$). WXRD analysis of the nanomaterials indicates that the anionic surfactant effectively penetrates into the polypyrrole chains, and a new peak at $2\theta = 6.3°$ (d-spacing = 14 Å) was observed corresponding to highly ordered polymer chains. UV−vis and FT-IR confirmed the highly doped state, and the conductivity of the samples was obtained in the range of 10^{-1} to 10^{-2} S/cm by four-probe conductivity measurements. The azobenzenesulfonic acid anionic surfactant is luminescent in water, and its grafting on the polypyrrole nanospheres enhances the luminescent intensity with the quantum yield in the range of 2×10^{-3} to 3×10^{-4}.

Introduction

Polypyrrole nanomaterials have good electrical conductivity, environmental stability, and biocompatibility and find a wide range of applications in electronic and optical devices, chemical and electrochemical sensors, electrochromic devices, actuators, and field emission applications, etc.[1−10] Polypyrrole nanomaterials were synthesized using hard porous polymeric templates,[11,12] electro-spinning,[13] seeding technique,[14] electrochemical polymerization,[15,16] dispersion polymerization,[17] interfacial polymerization,[18] copolymer methodology,[19] or surfactant-assisted micelles.[20] The surfactant-assisted chemical route is particular interesting because of easy removal of templates after the polymerization, potential for large scale-up reactions, and ability to distribute reactants between the micellar and solvent phases, which direct the reaction pathways for specified size and shape of the nanomaterials.[21] Polystyrene-poly(2-vinylpyridine)[22] or polystyrene-poly(4-vinylpyridine) block copolymers,[23] and cationic[21,24−27] or anionic surfactants[28−38] were employed as templates for the polypyrrole nanomaterial. Cetyltrimethylammonium bromide and dodecyltrimethylammonium bromide were good examples for cationic surfactants, and nanofibers (or spheres) were prepared either in the presence of dopant-like HCl or under neutral conditions.[24−26] In general, it was noticed that the removal of the cationic or neutral surfactant molecules during the purification step significantly influences the properties of the nanomaterials such as solubility, conductivity, and processability. On the other hand, anionic surfactants are very attractive for polypyrrole because they behave both as surfactant for polymerization as well as counteranion dopant for the positively charged polypyrrole matrix.[29] The anionic surfactants permanently bind to the polymer chains and become part of the resultant nanomaterials, and thus the properties of polypyrrole nanomaterials were maintained even after purification via standard protocols.[30,31] Polypyrrole nanotubes, nanofibers, and nanospheres were synthesized using anionic surfactants such as bis(2-ethylhexyl)sulfosuccinate,[20,30] sodium dodecyl sulfate,[32] dodecylbenzenesulfonicacid,[29,33] azobenzenesulfonic acid,[34] and β-naphthalenesulfonic acid.[35−37] Most often, the synthesis of polypyrrole nanomaterials using anionic surfactants was found very sensitive to the pyrrole/surfactant ratio, and good quality of nanomaterials was produced for only a few selective compositions.[34,36,37] The reason for the inhomogeneity in the nanomaterials formation was associated to the poor micelles formation of the anionic surfactants with pyrrole in water.[36] Unlike in the case of cationic surfactants, unfortunately, the mechanism of the anionic surfactant-mediated polypyrrole synthesis was not investigated in detail, which is a very crucial factor for reproducible nanomaterials synthesis.[39,40] It is very important to stabilize the micelles in water and understand their polymerization mechanism for precise control of polypyrrole

* Corresponding author. Fax: 0091-471-2491712. E-mail: jayakannan18@yahoo.co.in.

10.1021/jp0752670 CCC: $37.00
Published on Web 10/18/2007

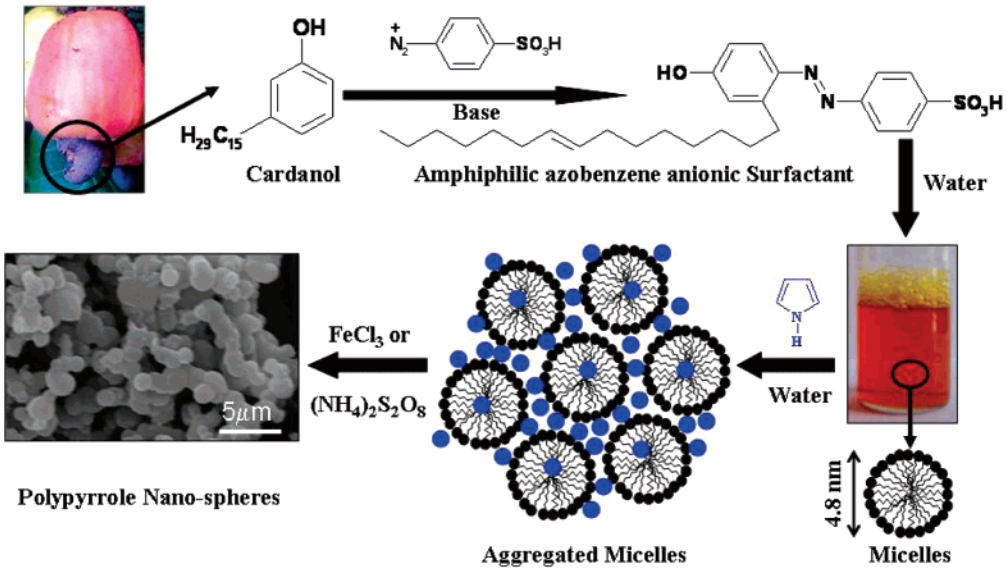

Figure 1. Synthesis of polypyrrole nanomaterials via anionic azobenzenesulfonic acid surfactant micellar-mediated self-organization process.

nanomaterial properties. Therefore, design and development of new amphiphilic anionic surfactant or dopant molecule is very much in need for the synthesis of polypyrrole nanomaterials with good solubility, morphology, high solid-state ordering, and precise control over the structure−property relationships.

We have reported a renewable resource strategy for size-controlled and highly ordered polyaniline nanomaterials via the self-assembly approach.[41,42] We have developed an idea of interconnecting both renewable resources and conducting nanomaterials because it is very new and has tremendous opportunities in the future for fundamental and applied research. A renewable resource raw material cardanol, which is an industrial waste and pollutant from cashew nut industry, is utilized for synthesizing new amphiphilic azobenzenesulfonic acid.[41] The sulfonic acid molecule was employed as a dopant for the polyaniline nanomaterials and various properties of polyaniline nanomaterials were controlled.[42] Recently, we have also developed a single molecular approach to selectively template polyaniline nanomaterials via interfacial and emulsion polymerization routes to control the polyaniline nanomaterials shape, size, solubility, solid-state ordering, and expanded polymer chain to coil-like conformation.[43] Here, we report, for the first time, a new series of water-soluble and highly ordered polypyrrole nanomaterials using a renewable resource amphiphilic azobenzenesulfonic acid derivative (see Figure 1) as an anionic surfactant. The composition of the pyrrole:anionic surfactant was varied from 1:1/3 to 1:1/100 (up to 100 times lower amount of surfactant with respect to pyrrole) in the feed, and the polypyrrole nanospheres were produced through controlled and self-organized micellar-mediated templates in water. Dynamic light scattering technique and specific viscosity measurements were employed as tools to trace the factors affecting the mechanism of the polypyrrole nanomaterials. The results revealed that the anionic surfactant exists in the form of 4.3 nm sized micelle in water. The interaction of surfactant with pyrrole produces aggregated micelles, which control the growth of the polypyrrole nanospheres. The role of the oxidizing agents was also investigated for the wider pyrrole:surfactant composition using ammonium persulfate (APS) and ferric chloride ($FeCl_3$). The polypyrrole nanospheres were characterized by SEM and TEM, UV−visible, and fluorescence spectroscopy, particle size analyzer, and wide-angle X-ray diffractions, etc. In a nut shell, in the present investigation, by carefully designing and understanding the mechanism of amphiphilic azobenzene anionic surfactant molecule, we have successfully prepared water-soluble and luminescent polypyrrole nanospheres with different sizes (100−800 nm) and high solid-state ordering in a single system via the self-assembly process.

Experimental Section

Materials. Pyrrole, ammonium persulfate (APS), sulfanilic acid, hydrochloric acid, ferric chloride hexahydrate, and sodium hydroxide were purchased locally and purified. Cardanol was purified by double-vaccum distillation at 3−4 mm of Hg, and the fraction distilled at 220−235 °C was collected.[41]

Measurements. NMR spectra of the compounds were recorded using a 300-MHz Brucker NMR spectrophotometer in d_6-dimethyl sulfoxide (DMSO) containing a small amount of tetramethylsilane (TMS) as the internal standard. Infrared spectra of the polymers were recorded using a Perkin-Elmer Precisely Spectrum One FT-IR spectrometer in the range of 4000−400 cm^{-1}. The purity of the compounds was determined by fast atom bombardment high-resolution mass spectrometry (FAB-HRMS:JOEL JSM600). For conductivity measurements, the polymer samples were pressed into a 10 mm diameter pellet and analyzed using a four-probe conductivity instrument by applying a constant current. The resistivities of the sample were measured at five different positions. For the SEM measurements, polymer samples were subjected to a thin gold coating using a JEOL JFC-1200 fine coater. The probing side was inserted into a JEOL JSM-5600 LV scanning electron microscope for taking photographs. WXRD of the finely powdered polymer samples was recorded by a Philips analytical diffractometer using Cu Kα emission. The spectra were recorded in the range of $2\theta = 0-40°$ and analyzed using X'Pert software. UV−vis spectra of the polypyrrole nanospheres were recorded using a Perkin-Elmer Lambda-35 UV−vis spectrometer. The thermal stability of polymers was determined by using a TGA-50 Shimadzu thermogravimetric analyzer at a heating rate of 10 °C per min in nitrogen. Fluorescence spectra of the samples were recorded using a Fluorolog F112X fluorimeter. The fluorescence quantum yields of the dopant and nanofibers were determined in water using quinine sulfate in 0.1 N sulfuric acid ($\phi = 0.546$) as standard by exciting at 360 nm. The concentration of polymer solution (also dopant) and standard was adjusted in such a

TABLE 1: Yield, Conductivity, Elemental Analysis, Dimensions of Nanospheres, and WXRD Data of Polypyrrole Nanomaterials

							WXRD data[g]	
sample[a]	conc. of surfactant (M^{-1})	surfactant: pyrrole (mol)[b]	yield[c] (%)	S/N ratio[d]	σ (S/cm)[e]	spheres[f] diameter (nm)	2θ values	d-spacing (Å)
P-3a	1.2×10^{-1}	1:3	27	0.34	0.001	coral-like	20.26	4.38
P-4a	9.0×10^{-2}	1:4	24	0.32	0.002	coral-like	20.04	4.43
P-5a	7.2×10^{-2}	1:5	23	0.30	0.02	150−220	9.02, 21.55	9.8, 4.12
P-10a	3.6×10^{-2}	1:10	23	0.29	0.04	180−220	8.96, 21.55	9.8, 4.12
P-25a	1.4×10^{-2}	1:25	38	0.26	0.01	180−220	7.66, 26.41	11.5, 3.37
P-50a	7.2×10^{-3}	1:50	29	0.25	0.01	180−220	6.87, 26.41	12.9, 3.37
P-75a	4.8×10^{-3}	1:75	30	0.26	0.02	180−220	6.86, 26.81	12.9, 3.32
P-100a	3.6×10^{-3}	1:100	33	0.25	0.02	180−220	6.23, 26.80	14.2, 3.31
P-5b	7.2×10^{-2}	1:5	51	0.32	0.83	500−1000	20.94	4.23
P-10b	3.6×10^{-2}	1:10	55	0.24	0.55	600−1200	26.04	3.96
P-25b	1.4×10^{-2}	1:25	58	0.21	0.06	600−1200	26.04	3.66
P-50b	7.2×10^{-3}	1:50	56	0.12	0.05	800−900	26.04	3.96
P-75b	4.8×10^{-3}	1:75	57	0.11	0.05	800−900	26.37	3.37
P-100b	3.6×10^{-3}	1:100	58	0.08	0.05	800−900	26.37	3.37

[a] Polypyrrole synthesized using ammonium persulfate (series-a) or $FeCl_3$ (series-b) as oxidizing agents. [b] Concentration of pyrrole was maintained as 3.6×10^{-1} M^{-1} for all of the polymerization reactions. [c] Yield calculated for isolated product. [d] Sulfur/nitrogen ratio was obtained by elemental analysis. [e] Conductivity was measured using a four-probe conductivity meter at 30 °C. [f] Diameter of the nanospheres was calculated from SEM images. [g] WXRD data were determined at 25 °C.

way to obtain the absorbance equal to 0.1 at 360 nm. The quantum yields of the samples were calculated via the following equation:[42]

$$\phi_s = \phi_r[F_s A_r / F_r A_s](n_r/n_s)^2$$

where ϕ_s is the fluorescence quantum yield of the sample, F is the area for the emission peak, n is the refractive index of solution, and A is the absorbance of the solution at the excitation wavelength. The subscripts r and s denote reference and sample, respectively. The resonance Raman peak for water appeared at 420 nm, which was deconvoluted computationally from the sample spectra for the calculating the area of the emission peaks. TEM analysis was recorded using a Hitachi H-600 instrument at 75 kV. For TEM measurements, a suspension of nanospheres was prepared in ethanol and deposited on a Formvar-coated copper grid. Viscosity was measured via an Automatic Ubbelohde viscometer (Schott). Particle analysis was done via a Malvern U.K. Zetasizer 3000 HAS, and DLS measurement was done via a Nano ZS Malvern instrument employing a 4 mW He−Ne laser ($\lambda = 632.8$ nm) and equipped with a thermostated sample chamber.

Synthesis of 4-[4-Hydroxy-2((*Z*)-pentadec-8-enyl)phenylazo]-benzenesulfonic Acid (Surfactant 1). Sulfanilic acid (6.9 g, 39.7 mmol) and sodium carbonate (1.6 g, 14.7 mmol) were dissolved in water (70 mL) by heating to 60−70 °C. It was then cooled to 5 °C, and a cold solution of sodium nitrite (2.4 g, 35.4 mmol) in water (8 mL) was added. The resultant yellow solution was poured into ice (50.0 g) containing concentrated HCl (8 mL) and stirred using a mechanical stirrer for 30 min at 5 °C. The cold diazonium salt was added dropwise into an aqueous solution containing cardanol (10.0 g, 33.1 mmol) and sodium hydroxide (4.0 g, 100 mmol) in water (30 mL). The reaction was continued with stirring for 3 h in the ice-cold conditions using a mechanical stirrer. The reaction mixture was neutralized by the addition of concentrated HCl (40 mL) in crushed ice (70.0 g). The red precipitate was filtered using a Buchner funnel and washed with water. The crude dried product (13.0 g) was further purified by passing through silica gel column using 5% methanol in ethyl acetate. The solvent was removed to obtain the product as a red-orange crystalline solid. Yield = 7.8 (49%). Melting point: 205−207 °C. ^{1}H NMR (d_6-*N*,*N*-DMSO) δ: 7.75 ppm (s, 4H, Ar−H), 7.57 ppm (d, 1H, Ar−H), 6.75 ppm (s, 1H, Ar−H), 6.70 ppm (d, 1H, Ar−H), 5.24 ppm (2H, CH=CH), 3.1−0.06 ppm (m, 29H, aliphatic-H). ^{13}C NMR (d_6-*N*,*N*-DMSO) δ: 161.25, 152.59, 149.14, 145.82, 142.98, 129.69, 126.75, 121.76, 116.88, 116.36, 114.23, 31.75, 31.24, 30.77, 29.14, 28.85, 28.59, 26.70, 26.62, and 25.33. FT-IR (KBr): 3006.7, 2923.6, 2852.9, 2852.9, 1600.1, 1533.7, 1498.7, 1369, 1338.7, 1263.9, 1174.7, 1116.5, 1033.2, 1007.6, 820.1, 706.4, and 559.3 cm^{-1}. UV−vis (in CH_3OH): λ_{max} = 336 nm. FAB-MS (MW: 486): $m/z = 486.3$ (M^+).

Preparation of Polypyrrole Nanospheres. A typical procedure for the preparation polypyrrole nanosphere is given for **P-100a**. The surfactant **1** (70 mg, 0.144 mmol) (for **P-100a**, pyrrole:surfactant is 1:1/100) was added to 25 mL of double distilled water in a 100 mL round-bottom flask and stirred for 15 min. Freshly distilled pyrrole (1 mL, 14.4 mmol) was added to the above solution and stirred for 45 min in ice-cold condition to obtain a dark red viscous solution. Ammonium per sulfate (0.9 g, 4 mmol) in 15 mL of double distilled water was added drop by drop to the above solution, and stirring was continued for 8 h under ice-cold condition. The resulting polypyrrole was purified by pouring into a large excess of distilled water, filtered, and washed with distilled water and methanol until the filtrate become colorless. The black powder sample was dried under vacuum (0.1 mm of Hg) for 12 h prior to further analysis. Yield = 33 (%). FT-IR (cm^{-1}): 1540, 1460, 1360, 1295, 1190, 1172, 1090, 1036, 960, 905, 783, 670, and 612.

A similar procedure was adopted in varying the amount of pyrrole:surfactant from 1:1/3 to 1:1/75 using APS as oxidizing agent to prepare polypyrrole nanomaterials **P-3a** to **P-75a** (**a**-for APS-series). Alternatively, ferric chloride (14.4 mol, 3.9 g) was employed as oxidizing agent instead of APS for pyrrole: surfactant ratio from 1:1/5 to 1:1/100 to prepare polypyrrole nanomaterials **P-5b** to **P-100b** (**b**- for $FeCl_3$-series). The yield, elemental analysis, and compositions of the reactants in the feed were summarized in Table 1.

Results and Discussion

A naturally occurring phenolic compound cardanol, which is an industrial waste and pollutant from the cashew nut processing industry, was utilized to develop a novel water-

soluble and anionic amphiphilic surfactant 4-[4-hydroxy-2((*Z*)-pentadec-8-enyl)phenylazo]-benzenesulfonic acid (named as surfactant **1**, see Figure 1). The structure of the azobenzene sulfonic acid was confirmed via NMR, FT-IR, and mass techniques (see Supporting Information). The surfactant **1** has unique built-in amphiphilic design in which the hydrophilic sulfonic acid behaves as polar head and the long alkyl chain as hydrophobic tail. The new surfactant **1** is freely soluble in water and various water loving organic solvents, which are an added advantage for preparing polypyrrole nanostructures under the micellar-mediated self-organization approach (see Figure 1). The polypyrrole nanomaterials were synthesized by varying the pyrrole:surfactant composition over a wide range from 1: 1/3, 1:1/4, 1:1/5, 1:1/10, 1:1/25, 1:1/50, 1:1/75, to 1:1/100 (up to 100 mol less amount of surfactant with respect to pyrrole) in water at ambient conditions. The concentration of the pyrrole was fixed as 3.6×10^{-1} M^{-1} for all of the compositions, and the concentration of surfactant was varied by dissolving various amounts in water (1.2×10^{-1} to 3.6×10^{-3} M^{-1}, see Table 1). Typically, the polymerization was carried out by taking pyrrole and surfactant in water and was stirred using a mechanical stirrer under ice-cold conditions for 1 h. The resultant viscous red solution was oxidized by adding an aqueous solution of ammonium per sulfate or ferric chloride at 0−5 °C under a mechanical stirrer for 30 min. The polymerization was continued for 8 h, and the green nanomaterial was filtered and purified by washing with water and methanol until the filtrate became colorless. It was dried under vacuum for 24 h (0.05 mm of Hg) at 60 °C in a vacuum oven prior to further analysis. The polymers are denoted as **P-Xa** or **P-Xb**, where "X" corresponds to the pyrrole/dopant (in moles) in the feed and "a" and "b" represent the nanomaterials prepared using APS or $FeCl_3$ as oxidizing agents, respectively. The yield and composition of the polypyrrole nanomaterials **P-3a**−**P-100a** and **P-5b**−**P-100b** are summarized in Table 1. The polypyrrole nanomaterials were subjected to FT-IR analysis (see Supporting Information) to confirm the structure of the doped polymers. The FT-IR spectra have showed clear characteristic peaks at 1548 and 1466 cm^{-1} with respect to symmetric and antisymmetric aromatic ring-stretching modes.[21,29] The peaks at 1050 and 1300 cm^{-1} correspond to the C−H and C−N stretching vibrations, respectively.[30] The presence of two peaks at 1190 cm^{-1} was attributed to the SO_3^--aromatic ring-doped state of polypyrrole.[29] This peak was slightly shifted to higher wavenumbers in the case of APS oxidized sample as compared to that of $FeCl_3$ oxidized polypyrrole materials. This may be due to the overlapping of the S═O peak (1183 cm^{-1}) with the polypyrrole-doped structures.[29] The peak at 915 cm^{-1} corresponds to the O═S═O stretching vibration in the sulfonic acid groups of the dopant.[21] All of the IR peaks are in accordance with the expected structure and match that reported for polypyrrole nanomaterials. The degree of doping is obtained from the elemental analysis of the nanomaterials. The sulfur/nitrogen (S/N) ratios were summarized in Table 1 for all of the polymer samples. The S/N values match earlier reports of polypyrrole nanomaterials prepared using anionic surfactants.[29,30] As expected, the S/N ratio decreases with decreases in the surfactant amount in feed, and values were obtained in the range of 0.34−0.25 and 0.32−0.08 for series-"a" and -"b", respectively. The samples prepared using APS have much higher S/N values as compared to $FeCl_3$, which is assigned to the presence of sulfate counterion in the former case.[29] The thermal analysis of the polypyrrole samples was analyzed by thermogravimetric analysis, and the polypyrrole samples doped by the new amphiphilic surfactant possess thermal stability up to 320 °C (see Supporting Information). Li et al. had recently reported high thermal stability for pyrrole−ethylaniline copolymer series, and interestingly in the present investigation the polypyrrole nanospheres also showed a very high thermal stability as reported earlier.[44]

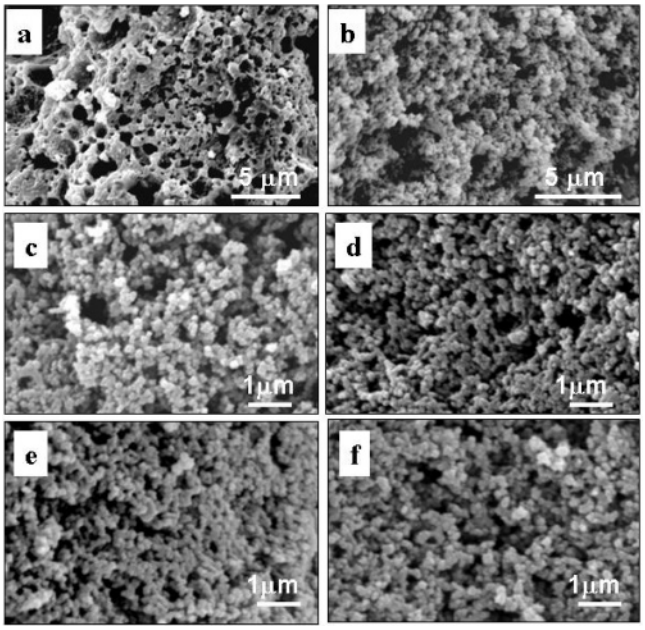

Figure 2. SEM pictures of polypyrrole nanomaterials prepared using APS as oxidizing agent (series-a): **P-3a** (a), **P-5a** (b), **P-25a** (c), **P-50a** (d), **P-75a** (e), and **P-100a** (f).

The morphologies of the nanomaterials were recorded using a JEOL JSM-5600 LV scanning electron microscope, and SEM images of the polypyrrole samples are given in Figure 2. The anionic azobenzenesulfonic acid surfactant-mediated polypyrrole nanomaterials were highly sensitive to the pyrrole:surfactant ratio, and different morphologies were produced depending upon their amount in the feed. At higher surfactant concentration (1.2×10^{-1} to 9.0×10^{-2} M^{-1}) (for **P-3a**−**P-5a**), the pyrrole−surfactant complex was found as solution plus precipitate in water, which lead to the formation of coral-like morphology (see vials in the Supporting Information). As the surfactant amount further decreases in the feed (3.6×10^{-2} to 3.6×10^{-3}, from **P-10a** to **P-100a**), the reaction mixture was found more homogeneous, which resulted in the formation of uniform polypyrrole nanospheres of diameter in the range of 150−250 nm. SEM images of polypyrrole nanomaterials produced using $FeCl_3$ as oxidizing agent under the identical conditions were shown in Figure 3. The sample **P-5b** has spheres plus coral-like morphology, whereas the samples **P-10b**−**P-100b** have predominantly 0.5−0.9 submicrometer spheres. However, the diameters of the nanospheres were much higher for series-a (prepared using APS) as compared to series-b (prepared using $FeCl_3$). SEM technique has limitation for very small size nanomaterials (<150 nm range), which account for the poor resolution of SEM images for series-a samples (small spheres) in Figure 2.[25] The samples were subjected for transmission electron microscopic (TEM) analysis to obtain better morphology of these nanomaterials. TEM images of **P-50a** and **P-100b** are shown in Figure 4. TEM images of the samples clearly indicate that the materials have uniform solid nanospheres (no hollow spheres or fibers) and their diameters are in the range of 150 and 800 nm for **P-50a** and **P-100b**, respectively. The comparison of the TEM and SEM images of these samples reveals that the nanospheres diameters are almost comparable in both techniques. It suggests that the specially designed

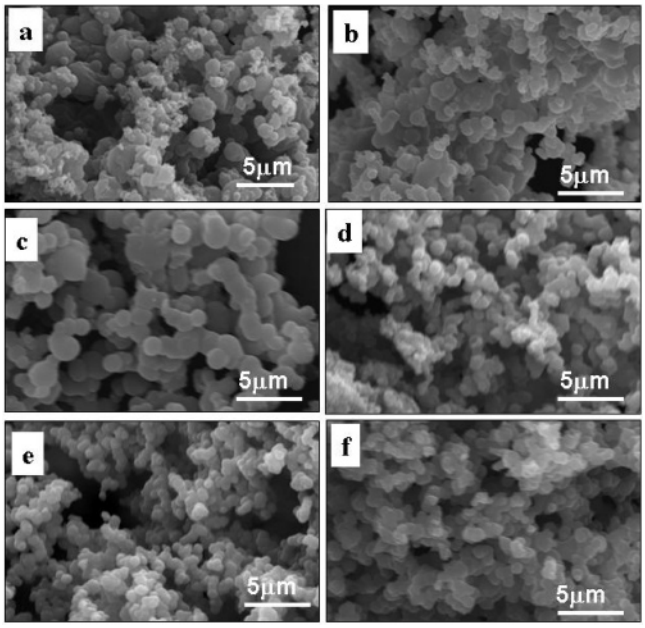

Figure 3. SEM pictures of polypyrrole nanomaterials prepared using $FeCl_3$ as oxidizing agent (series-b): **P-5b** (a), **P-10a** (b), **P-25b** (c), **P-50b** (d), **P-75b** (e), and **P-100b** (f).

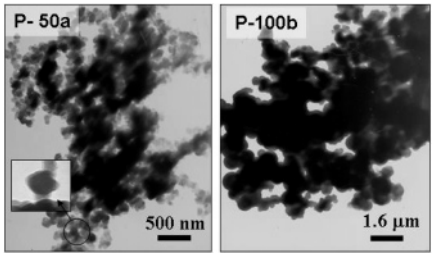

Figure 4. TEM pictures of polypyrrole nanomaterials.

renewable resource amphiphilic molecule is a very efficient anionic surfactant for polypyrrole, and, for the first time, we have shown that the size and nature of the nanomaterials can be fine-tuned for a wide composition range of pyrrole:dopant in the feed. Although there is a difference in the sizes of the nanospheres produced by oxidizing agents, interestingly both routes produced only nanospheres and no traces of fibers were found in the materials. It indicates that the mechanism of the nanospheres formation is mainly controlled by the surfactant−pyrrole complexes in water rather than the types of the oxidizing agents employed. It is quite opposite to the observations reported by Wu et al.[24] and Zhang et al.[21] in the cetyltrimethylammonium bromide (CTAB) cationic surfactant-mediated polypyrrole synthesis. They found that $FeCl_3$ oxidation of CTAB−pyrrole complex produced spheres, whereas wire-like network morphology was obtained for APS oxidation.[21] Recently, Li et al. studied the mechanistic aspects of the pyrrole/4-sulfonic diphenylamine copolymer system and found that the size of the copolymer particles formed is greatly influenced by the monomer composition and their distribution in the initial stages.[19] Interestingly, in the present system, neither change in the amount of pyrrole:surfactant ratio (for wide range of 1:1/5 to 1:1/100 in the feed) nor oxidizing agent disturb the morphology of the nanomaterials. It is very surprising to notice that nanospheres were produced even at very low concentration of the surfactant, which is almost 1/100 lower than that of pyrrole in the feed. It indicates that the anionic surfactant-mediated synthesis of polypyrrole nanomaterials follows a quite different pathway as compared to that of the cationic surfactants reported by others. Therefore, it is very important to study the behavior of the amphiphilic surfactant and surfactant+pyrrole complex in water to understand the formation of nanomaterials.

In the emulsion polymerization route, the shape and dimensions of the nanomaterials are highly dependent on their micellar state, and these micelles either in the isolated or in the aggregated state determine the properties of the resultant nanomaterials such as their size, length, and type.[39] Recently, during the course of tracing the mechanistic aspects in the synthesis of polyaniline nanomaterials using the same azobenzenesulfonic acid by fluorescence spectroscopy, we found that the renewable resource anionic surfactant was highly luminescent for excitation at 360 nm.[42] The azo-benzene molecule was found to exist in either aggregated or isolated supramolecular aggregates such as micelles depending upon its concentration in water. To confirm the existence of micellar behavior, in the present investigation, the surfactant was subjected to dynamic light scattering (DLS) studies in water. The surfactant was dissolved in water (1×10^{-3} M^{-1}, a similar concentration range of the surfactant used for polymer synthesis, see Table 1), and DLS data are shown in Figure 5. DLS revealed that more than 99.4% of the azobenzene surfactant molecule in water exists in the form of the micelles, and their average diameters were obtained as 4.29 nm. The theoretical size of the surfactant molecule was calculated using AM1 calculations and found that the end-to-end distance of the polar head to hydrophobic tail was obtained as 24.4 Å or 2.44 nm (see Figure 5). The diameter of the tightly packed spherical surfactant is always equal to double the size of the molecule. The theoretical diameter of the micelle is equal to 2×2.44 nm $= 4.88$ nm, which almost matches that of the values obtained experimentally by DLS. It confirms that the new renewable resource-based azobenzene sulfonic acid derivatives are a good anionic surfactant and form stable spherical micelles in water. Our attempts to trace the micellar behavior of the pyrrole+surfactant complexes in water by DLS technique were hampered due to the strong red absorption of the mixture in water.[39] To identify the behavior of pyrrole+surfactant complexes, we have utilized solution viscosity technique, which is another powerful tool to trace the self-organization of secondary structures such as micelles and its interaction with molecules. We have measured the solution viscosity (specific) of pyrrole−surfactant complex in water using an automatic viscometer at 30 °C. The specific viscosity of the pyrrole−surfactant complex is plotted against the ratio of the concentration of [pyrrole]/[dopant] in the feed and shown in Figure 6. The specific viscosity of the neat azobenzenesulfonic acid surfactant is negligible, which indicates that micelles are almost in an isolated state in water. Upon adding pyrrole, the viscosity of the solution significantly increases, which is attributed to the formation of larger size micellar aggregates of anionic surfactant micelles (acidic) with pyrrole molecules (as basic). The gradual decrease in the viscosity plot followed by the decrease in the amount of surfactant in the complex is due to the reduction in the numbers of micelles and also the formation of weakly aggregated micelles (see Figure 6). The specific viscosity measurements revealed that at higher surfactant concentration the complex exists in the form of strong aggregated micelles and oxidation of these aggregated templates produced coral-like morphology in **P-3a**−**P-5a** and **P-5b** (see Figures 2 and 3). On the other hand, at lower surfactant concentration the weakly aggregated micelles produced well-defined polypyrrole nanospheres of 150−800 nm. Because both oxidizing agents produced only nanospheres (no traces of the nanofibers), it confirms that the self-organization of the sur-

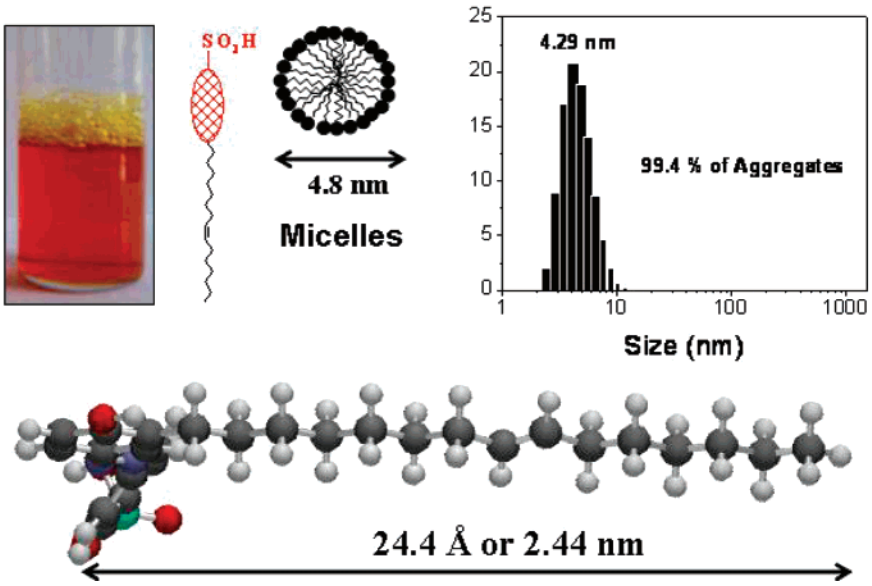

Figure 5. DLS data of the anionic surfactant and AM1 energy-minimized structure.

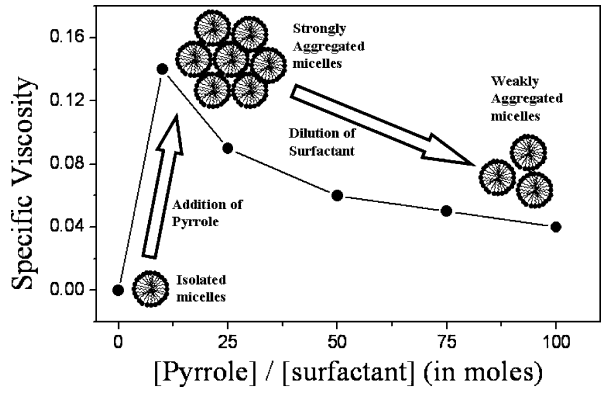

Figure 6. Specific viscosity of the anionic surfactant+pyrrole complex and possible micellar aggregated templates.

factant−pyrrole complex plays a major role in determining the morphology of the nanomaterials rather than the oxidizing agents.

To further support the above mechanism, the polypyrrole nanospheres **P-50a**, **P-75a**, and **P-100a** were dispersed in water and subjected to particle size analysis. The nanoparticle sizes and their distribution are plotted and shown in Figure 7. **P-50a** has two distributions with average diameter of the nanospheres centered at 400 nm and 1.6 μM. **P-75a** has also showed a broad distribution centered at 450 nm, but the average particle size is much lower than that of **P-50a**. Interestingly, the nanospheres were found very uniform in the case of **P-100a** with average diameter of 300 nm. The average size of the nanospheres determined by this method is almost comparable to that of SEM and TEM. The change in the bi-model (in **P-50a**) to broad (**P-75a**) to uniform distribution (in **P-100**) of nanospheres in Figure 7 supports the transformation of pyrrole−surfactant templates from strongly aggregated to isolated stage depending upon the concentration of the surfactant in the feed. The comparisons of data from the viscosity, particle size, and morphology of the samples revealed that at higher surfactant concentration the pyrrole−surfactant exists in the form of aggregated micelles, which lead to coral-like morphology or broad distribution of nanospheres, whereas at dilute conditions the complex produced well-defined uniform polypyrrole nanospheres. In the present investigation, we have demonstrated that by controlling the micellar behavior of the pyrrole+anionic surfactant complex

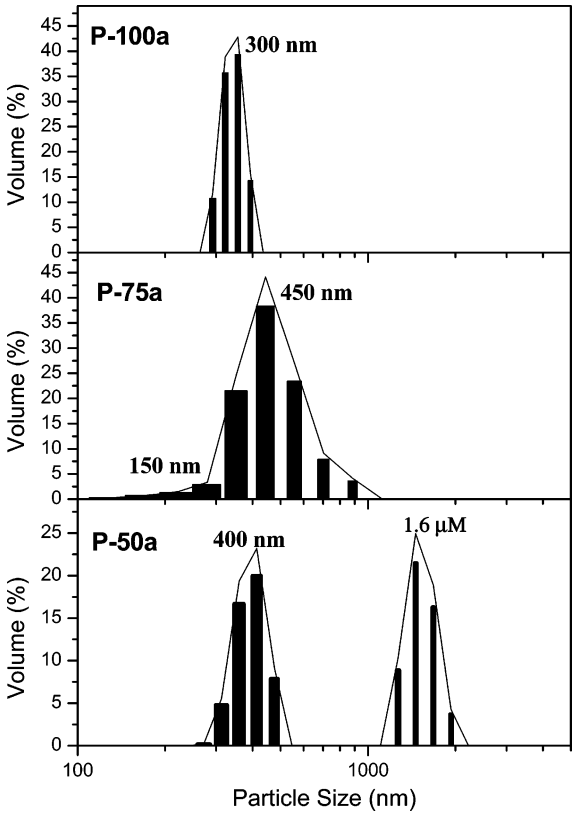

Figure 7. Particle size distribution of polypyrrole nanospheres.

in the feed, one can precisely control the morphologies of the polypyrrole nanomaterials.

The polypyrrole nanomaterials were freely suspended in water by stirring under ultrasonic at room temperature. Polypyrrole nanomaterials prepared using APS as oxidant were found to be more dispersible in water, whereas the samples prepared using $FeCl_3$ were insoluble and less dispersible in water. UV−visible spectra of the samples **P-3a**−**P-100a** were recorded in water and shown in Figure 8 (spectra for **P-5b**−**P-100b** are shown in the Supporting Information). The absorption spectra of azobenzenesulfonic acid surfactant showed strong transition at 360 and a shoulder at 450 nm corresponding to the $\pi-\pi^*$ and $n-\pi^*$ transitions of trans and cis azobenzene isomers.[42] The UV−

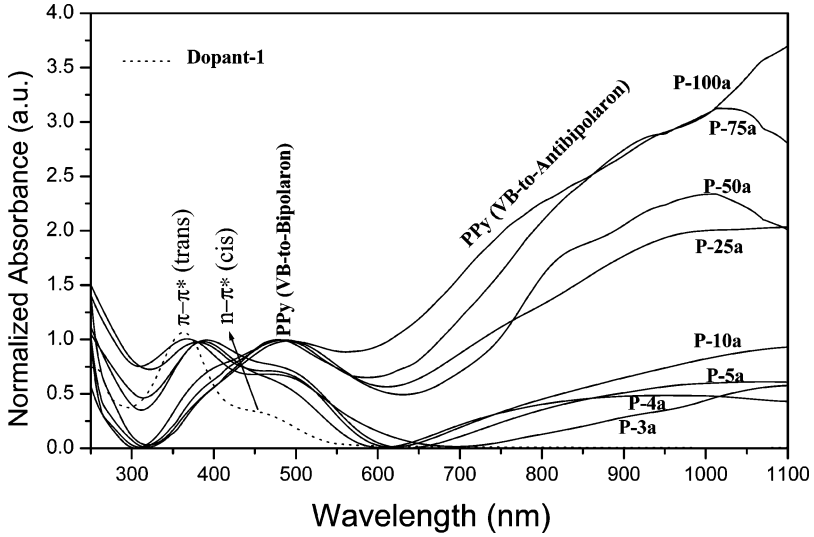

Figure 8. UV−vis absorbance spectra of surfactant and polypyrrole nanomaterials in water.

visible spectra of polypyrrole nanomaterials showed three distinct bands at 400 nm, 475 nm, and a free tail above 1000 nm in the NIR region.[11,45] These three transitions corresponded to the transitions from valence bond to polarons, bipolarons, and anti-bipolarons of the oxidized form of polypyrrole.[11] The increase in the intensity of the low-energy transition in the NIR for samples **P-25a**−**P-100a** revealed that these nanomaterials were highly doped as compared to that of the **P-3a**−**P-10a**. The conductivity of the polypyrrole nanostructures was determined by four-probe conductivity measurement for compressed pellets at room temperature (see Table 1). The conductivity values for the samples **P-5a**−**P-100a** were obtained in the range of 1×10^{-2}, whereas **P-3a** and **P-4a** showed 1 order lower conductivity as compared to other samples. The low conductivity of samples **P-3a** and **P-4a** reflects on their UV−vis spectra (Figure 8) that these samples have weak peaks corresponding to the bipolaron transitions as compared to **P-10a**−**P-100a**. Additionally, the morphology of the **P-3a**−**P-5a** was also highly porous (see Figure 2), which may also be accountable for their low conductivity.[41] The polymers **P-5b**−**P-100b** prepared using $FeCl_3$ showed much higher conductivity (up to the range of 1×10^1) as compared to the APS-series. Li et al. reported[44] the conductivity of HCl-doped polypyrrole copolymer microspheres (using APS as oxidant) in the range of 10^{-1}, which is 1 order higher than that of polypyrrole nanospheres (150−220 nm) obtained in the present system for the same oxidizing agent (see series-a in Table 1). It may be due to the difference in the doping ability of aromatic sulfonic acid as compared to that of the inorganic acids such as HCl.[29] A similar observation was reported by Omastova et al., and these differences in the conductivity values were attributed to the counterion effect of the oxidizing agents.[29] Because the amphiphilic azobenzene sulfonic acid surfactant is luminescent in water (described in detail in the earlier report),[42] its grafting effect on the polypyrrole nanofibers was studied in water. The emission spectra were recorded followed by exciting at 360 nm corresponding to the $\pi-\pi^*$ (trans) of the azobenzene part in the surfactant. The emission spectra for the surfactant and few representative nanomaterials were shown in Figure 9. The resonance Raman peak for water (as a solvent) at 420 nm is very intense because of the low concentration of the molecules in water.[42] The nanomaterials showed a broad peak at 450 nm corresponding to the luminescence of azo-groups, which is well separated from the water Raman peak. The luminescence intensity of the nanomaterials drastically decreases with the decrease in surfactant concentration in the feed. The quantum yield of the nanofibers was obtained using quinine sulfate as reference in water and is shown in Figure 9 (see inset). The quantum yield of the surfactant was obtained as 2.6×10^{-3}, which is in the same range as reported for azobenzene amphiphilic chromophores. It suggests that the amount of the dopant present in the nanomaterial is very crucial for obtaining highly luminescent (also quantum yield) polypyrrole materials based on the renewable resource anionic surfactant. More detailed studies on the aggregation behavior of these nanofibers in aqueous or organic medium are currently in progress.

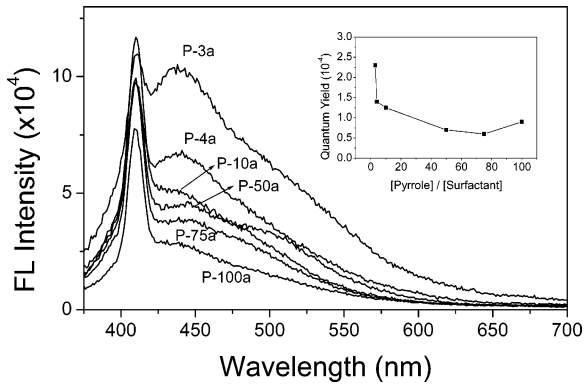

Figure 9. Emission spectra of polypyrrole nanospheres in water for excitation at 360 nm. The peak at 420 nm corresponds to the resonance Raman for water solvent. The inset provides the data for the quantum yield.

The solid-state properties of polypyrrole nanospheres were studied for finely powdered samples using wide-angle X-ray diffraction analysis (WXRD). Polypyrrole is a highly rigid polymer because of its linear structure and less flexible chain folding to induce crystalline domain. In the presence of organic surfactants, the dopant-polymer undergoes various interactions, which tend to organize the polymer chains in three-dimensional highly ordered fashions.[46] The WXRD patterns of polypyrrole nanospheres were shown in Figure 10. In Figure 10a, the WXRD patterns showed two characteristic peaks in the regions at $2\theta = 20-26°$ (d-spacing 4.12−3.32 Å) and $2\theta =$ below 10° (d-spacing = 11.5−14.2 Å). Decreasing the amount of surfactant drastically affects the nature of the peaks in the WXRD plots. While moving from **P-5a** to **P-100a**, the peak at $2\theta = 20°$ showed shift toward higher angle (from $2\theta = 20.04°$ to 26.37°), whereas the peak at $2\theta = 10°$ showed an opposite trend, that

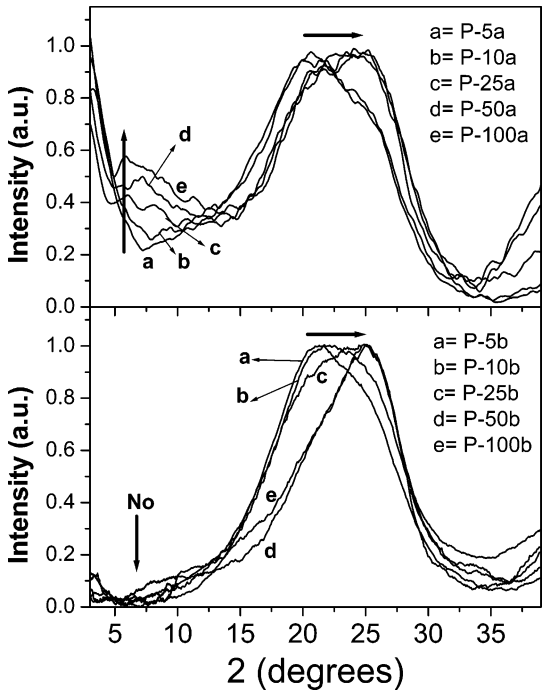

Figure 10. WXRD spectra of the polypyrrole nanomaterials.

is, toward lower angle (from $2\theta = 9.1-6.3°$). The peaks centered at $2\theta = 20.04°$ (d-spacing = 4.43 Å) and 26.37° (d spacing = 3.37 Å) are assigned to scattering from pyrrole−counterion or inter-counterion interactions and pyrrole−pyrrole inter-planar distance.[47,48] The shift from 4.43 to 3.37 Å in the higher angle region may be due to the difference in the doping level and related to the pyrrole−pyrrole and pyrrole−counterions. The lower angle peak (d-spacing = 14.2 Å) is particular very interesting because both the intensity as well as the inter-planar distance (d-spacing values) increase while moving from **P-25a** to **P-100a**. It indicates that the decrease in the amount of surfactant in the feed increases the inter-planar distance in the nanomaterials and produces highly ordered polypyrrole nanospheres. Surprisingly, the $FeCl_3$-series samples did not show any significant peak in the low-angle region. It suggests that the samples **P-25b**−**P-100b** are poorly ordered, and it may be the reason for the low solubility of these samples as compared to that of the **P-25a**−**P-100a** in water. In **P-3a**−**P-100a**, the penetration of the surfactant molecule increases the inter-planar distance, and, therefore, the solvent molecules easily enter into the lattices to dissolve the polymer chain in water. Currently, the work is in progress to study the effect of structural difference in the surfactant molecule on the solubility, ordering, and other properties of polypyrrole nanomaterials, which will be published elsewhere.

Conclusion

In conclusion, we have developed a renewable resource amphiphilic azobenzene sulfonic acid and utilized it as an anionic surfactant for water-soluble, luminescent, highly solid-state ordered, and uniform size polypyrrole nanospheres. The present approach is demonstrated for a larger window of pyrrole: surfactant ratio in the feed from 1:1/3 to 1:1/100 (using surfactant up to 100 times lower than that of pyrrole), for the first time, to systematically control the aggregation of pyrrole+surfactant micelles for tuning the properties of polypyrrole nanomaterials. The present approach has many advantages: (i) a new renewable resource anionic surfactant was synthesized and utilized as structure-directing agent for tuning the properties of polypyrrole nanomaterials. (ii) The surfactant molecule exists in the form of spherical micelles of 4.8 nm diameter and has a tendency to form a stable pre-template aggregate with pyrrole for a wider composition of pyrrole:surfactant from 1:1/3 to 1:1/100 in the feed, which is very rarely reported in the literature. (iii) The anionic surfactant has built-in head-to-tail amphiphilic nature for producing highly ordered polypyrrole nanospheres, and its presence enhances the solubility of the nanomaterials in water and organic solvents such as dimethylformamide, etc. (iv) The mechanism of the nanospheres formation was understood using dynamic light scattering techniques and solution viscosity measurements. (v) The surfactant is very cheap and can be easily synthesized from the naturally available resource cardanol, the main component of cashew nut shell liquid. The surfactant has free phenolic group, and we are currently developing new chemistry to substitute long-chain hydrophilic or hydrophobic units. These molecules will be utilized to fine-tune the polypyrrole nanostructured materials, which will be published elsewhere. In a nut shell, in the present investigation, polypyrrole nanospheres with water solubility, luminescent, and solid-state ordering were precisely controlled in a single system by understanding the mechanism of the new anionic surfactant-mediated pre-template self-assembly process.

Acknowledgment. We thank the Department of Science of Technology, New Delhi, India, under Schemes DST/TSG/ME/2005/33 and NSTI Programme-SR/S5/NM-06/2007, KSCTSE, Thiruvananthapuram, Kerala, India (082/SRSPS/2004/CSTE), for financial support. We thank Dr. Peter Koshy, Mr. M. R. Chandran, Dr. U. Syamaprasad, and Mr. P. Gurusamy, NIIST-Trivandrum, for SEM and WXRD analysis. We also thank Dr. Annie John, SCTIMST, Trivandrum, for TEM analysis. M.J.A. thanks UGC-New Delhi, India, for a junior research fellowship.

Supporting Information Available: Additional information for the synthesis and characterization of the surfactant, FT-IR spectra of the nanomaterials, TGA plots, vials containg the solution of surfactant and surfactant+pyrrole complex, and UV−vis spectra of series-b nanomaterials. This material is available free of charge via the Internet at http://pubs.acs.org.

References and Notes

(1) Wallace, G. G.; Kane-Maguire, L. A. P. *Adv. Mater.* **2002**, *14*, 953.
(2) Berdichevsky, Y.; Lo, Y. *Adv. Mater.* **2006**, *18*, 122.
(3) Otero, T. F.; Cortes, M. T. *Adv. Mater.* **2003**, *15*, 279.
(4) Wang, J.; Jiang, M. *Langmuir* **2000**, *16*, 2269.
(5) Bidon, G.; Billion, M.; Livache, T.; Mathis, G.; Roget, A.; Torres-Rodriguez, M. *Synth. Met.* **1999**, *102*, 1363.
(6) Girotto, E. M.; De Paoli, M. *Adv. Mater.* **1998**, *10*, 790.
(7) Korri-Youssoufi, H.; Garnier, F.; Srivastava, P.; Godillot, P.; Yassar, A. *J. Am. Chem. Soc.* **1997**, *119*, 7388.
(8) Ramanathan, K.; Bangar, M. A.; Yun, M.; Chen, W.; Myung, N. V.; Mulchandani, A. *J. Am. Chem. Soc.* **2005**, *127*, 496.
(9) Cosnier, S. *Electroanalysis* **2005**, *17*, 1701.
(10) Yoon, H.; Chang, M.; Jang, J. *J. Phys. Chem. B* **2006**, *110*, 14074.
(11) Menon, V. P.; Lei, J.; Martin, C. R. *Chem. Mater.* **1996**, *8*, 2382.
(12) Ikegame, M.; Tajima, K.; Aida, T. *Angew. Chem., Int. Ed.* **2003**, *42*, 2154.
(13) Kang, T. S.; Lee, S. K.; Joo, J.; Lee, J. Y. *Synth. Met.* **2005**, *153*, 61.
(14) Zhang, X.; Manohar, S. K. *J. Am. Chem. Soc.* **2005**, *127*, 14156.
(15) Qu, L.; Shi, G.; Chen, F.; Zhang, J. *Macromolecules* **2003**, *36*, 1063.
(16) Lu, G.; Li, C.; Shi, G. *Polymer* **2006**, *47*, 1778.
(17) Acik, M.; Baristiran, C.; Sonmez, G. *J. Mater. Sci.* **2006**, *41*, 4678.
(18) Vito, S. D.; Martin, C. R. *Chem. Mater.* **1998**, *10*, 1738.
(19) Li, X. G.; Wei, F.; Huang, M. R.; Xie, Y. B. *J. Phys. Chem. B* **2007**, *111*, 5829.
(20) (a) Jang, J.; Yoon, H. *Langmuir* **2005**, *21*, 11484. (b) Jang, J.; Yoon, H. *Chem. Commun.* **2003**, 720.

(21) Zhang, X.; Zhang, J.; Song, W.; Liu, Z. *J. Phys. Chem. B* **2006**, *110*, 1158.
(22) Goren, M.; Lennox, R. B. *Nano Lett.* **2001**, *1*, 735.
(23) Yoo, S. I.; Sohn, B.; Zin, W. C.; Jung, J. C. *Langmuir* **2004**, *20*, 10734.
(24) Wu, A.; Kolla, H.; Manohar, S. K. *Macromolecules* **2005**, *38*, 7873.
(25) Zhong, W.; Liu, S.; Chen, X.; Wang, Y.; Yang, W. *Macromolecules* **2006**, *39*, 3224.
(26) Jang, J.; Yoon, H. *Small* **2005**, *12*, 1195.
(27) Jang, J.; Oh, J. H.; Stucky, G. D. *Angew. Chem., Int. Ed*. **2002**, *41*, 4016.
(28) DeArmitt, C.; Armes, S. P. *Langmuir* **1993**, *9*, 652.
(29) Omastova, M.; Trchova, M.; Kavarova, J.; Stejskal, J. *Synth. Met.* **2003**, *138*, 447.
(30) Omastova, M.; Trchova, M.; Pionteck, J.; Prokes, J.; Stejskal, J. *Synth. Met.* **2004**, *143*, 153.
(31) Stejskal, J.; Omastova, M.; Fedorova, S.; Prokes, J.; Trchova, M. *Polymer* **2003**, *44*, 1353.
(32) Shen, Y.; Wan, M. *Synth. Met.* **1998**, *96*, 127.
(33) Lee, J. Y.; Kim, D. Y.; Kim, C. Y. *Synth. Met.* **1995**, *74*, 103.
(34) Haung, K.; Wan, M.; Long, Y.; Chen, Z.; Wei, Y. *Synth. Met.* **2005**, *155*, 495.
(35) Wei, Z.; Zhang, L.; Yu, M.; Yang, Y.; Wan, M. *Adv. Mater*. **2005**, *15*, 1382.
(36) Liu, J.; Wan, M. *J. Mater. Chem.* **2001**, *11*, 404.
(37) Shen, Y.; Wan, M. *J. Polym. Sci., Part A: Polym. Chem.* **1997**, *35*, 3689.
(38) Cassignol, C.; Olivier, P.; Richard, A. *J. Apply. Polym. Sci.* **1998**, *70*, 1567.
(39) Zhang, X.; Kolla, H. S.; Wang, X.; Raja, K.; Manohar, S. K. *Adv. Funct. Mater.* **2006**, *16*, 1145.
(40) Carswell, A. D. W.; O'Rear, E.; Grady, B. P. *J. Am. Chem. Soc.* **2003**, *125*, 14793.
(41) Anilkumar, P.; Jayakannan, M. *Langmuir* **2006**, *22*, 5952.
(42) Anilkumar, P.; Jayakannan, M. *J. Phys. Chem. C* **2007**, *111*, 3591.
(43) Anilkumar, P.; Jayakannan, M. *Macromolecules* **2007**, *40*, 7311.
(44) Li, X. G.; Huang, M. R.; Zhu, M. F.; Chen, Y. M. *Polymer* **2004**, *45*, 385.
(45) Cabala, R.; Skarda, J.; Potje-Kamloth, K. *Phys. Chem. Chem. Phys.* **2002**, *2*, 3283.
(46) Jayakannan, M.; Annu, S.; Ramalekshmi, S. *J. Polym. Sci., Part B: Polym. Phys*. **2005**, *43*, 1321.
(47) Wernet, W.; Monkenbusch, M.; Wegner, G. *Macromol. Chem. Rapid Commun*. **1984**, *5*, 157.
(48) Song, M. K.; Kim, Y. T.; Kim, B. S.; Kim, J.; Char, K.; Rhee, H. W. *Synth. Met.* **2004**, *141*, 315.